Chem Soc Rev

Interfacial Phenomena in Gas Hydrate Systems

SCHOLARONE™
Manuscripts

Chemical Society Reviews

ARTICLE

Interfacial Phenomena in Gas Hydrate Systems

Zachary M. Aman[a]* and Carolyn A. Koh[b]*

Gas hydrates are crystalline inclusion compounds, where molecular cages of water trap lighter species under specific thermodynamic conditions. Hydrates play an essential role in global energy systems, as both a hinderance when formed in traditional fuel production and a substantial resource when formed by nature. In both traditional and unconventional fuel production, hydrates share interfaces with a tremendous diversity of materials, including hydrocarbons, aqueous solutions, and inorganic solids. This article presents a state-of-the-art understanding of hydrate interfacial thermodynamics and growth kinetics, and the physiochemical controls that may be exerted on both. Specific attention is paid to the molecular structure and interactions of both water, guest molecules, and hetero-molecules (e.g., surfactants) near the interface. Gas hydrate nucleation and growth mechanics are also presented, based on studies using a combination of molecular modeling, vibrational spectroscopy, and x-ray and neutron diffraction. The fundamental physical and chemical knowledge and methods presented in this review may be of value in probing parallel systems of crystal growth in solid inclusion compounds, crystal growth modifiers, emulsion stabilization, and reactive particle flow in solid slurries.

Introduction

Clathrate hydrates (hereinafter "hydrates") are crystalline inclusion compounds, where molecular cages of water surround species with low molecular weight (e.g. methane).[1] Hydrates were first discovered by Sir Humphry Davy in 1810, and remained a laboratory curiosity for more than a century. In 1934, Hammerschmidt identified the existence of hydrates in industrial gas flowlines, where particle build-up enabled line blockage.[2] This industrial challenge remains today, where substantial hydrate-related research focuses on the prevention of blockages in hydrocarbon flowlines.[3] Following a ground-breaking study in 1965, naturally-occurring hydrates have received substantial focus as the largest global hydrocarbon resource discovered to date.[4] Prevalent along continental margins,[5] natural hydrates provide an attractive mechanism for gas storage (over 160 volumes of gas at standard temperature and pressure per volume of hydrate[6]). This property has elevated hydrates as a potential synthetic gas storage medium,[7] of particular interest are hydrogen, natural gas,[8] as well as carbon dioxide.

Over the past eight decades, hydrate research has been directed toward identifying the correct thermodynamic phase

[a.] University of Western Australia, School of Mechanical and Chemical Engineering, 35 Stirling Hwy M050, Crawley WA, 6009, AUSTRALIA.
[b.] Colorado School of Mines, Center for Hydrate Research, Department of Chemical and Biological Engineering, 1600 Illinois St, Golden CO, 80401, UNITED STATES.

* Corresponding authors: zachary.aman@uwa.edu.au, +61 8 6488 3078
  ckoh@mines.edu, +1 303 273 3237

boundaries,[1] with a minority focus on understanding the kinetic[9-11] or transport-limited[12] rates of crystal growth. While thermodynamic knowledge enables both the avoidance of hydrate growth in hydrocarbon transmission and the production of methane from natural methane hydrate reservoirs, thermodynamic control has been also used to promote hydrate growth for gas storage and transportation applications.

To date, three repeating crystal structures have been identified in conventional and unconventional energy applications: structure I (sI), structure II (sII), and structure H (sH). Each crystal structure utilises the smallest hydrate cavity – a pentagonal dodecahedron annotated as 5^{12} (12 pentagons in the faces of the small cage) – as the primary building block, which is complemented by a large cavity ($5^{12}6^2$, $5^{12}6^4$, and $5^{12}6^8$ for sI, sII, and sH, respectively).[13] The thermodynamically preferred crystal structure is dictated by a combination of temperature, pressure, and the availability of hydrate-forming guest components. The average large cage diameters of sI and sH are approximately 4.33 and 5.79 Å respectively, indicating sH is capable of enclathrating larger guest molecules (e.g. n-butane, methylcyclohexane) that are too large for the sI cavity[6].

The formation of hydrates from species with high vapour pressure (e.g. methane) requires a combination of high pressure and low temperature. These conditions are readily achieved in subsea conventional energy flowlines, where distributed hydrocarbons flow at high pressure with produced water; if the lines cool to sufficient temperature (typically below 300 K), gas hydrates may become stable. As such, significant effort has been expended to measure and model the thermodynamic boundaries of hydrate-forming gases. Beyond lookup tables, computational tools, such as Multiflash,[14] utilise cubic plus association (CPA) equations of state, where the fugacity of the solid hydrate phase is refined through comparison with laboratory data. Ballard et al.[15, 16] demonstrated the use of Gibbs Energy Minimisation as a tool to refine classical equations of state in predicting the hydrate phase boundary with a high degree of accuracy (< 0.53 K) for multicomponent hydrocarbon gasses.

In natural sediment systems,[17] hydrate may occur in three states:[18] (i) solid particles that share contact with grain boundaries, which partially bear the geomechanical load; (ii) small particles that occupy the pore space; and (iii) a coating layer at the grain-water interface that acts to cement the grains,[19] affecting the propagation of seismic waves through the sediment.[20, 21] The distributed nature of hydrate occurrence in natural systems highlights the importance of interfacial tension, which may dictate the optimal location of hydrate nucleation and growth. The formation and migration of gas hydrate through natural systems critically affects geomechanical sediment stability.[22] In these systems, hydrate may share an interfacial boundary with the sediment or pore fluid.

Figure 1 illustrates the five key concepts of gas hydrate interfacial phenomena: i) liquid-liquid and solid-liquid interfacial tension; ii) supersaturation of guest molecules across the interface; iii) hydrate-sediment interaction(s) relevant to porous media applications; iv) liquid-like characteristics near hydrate-hydrophobic boundaries; and v) surfactant adsorption to, and interaction with, hydrate-hydrophobic interfaces.
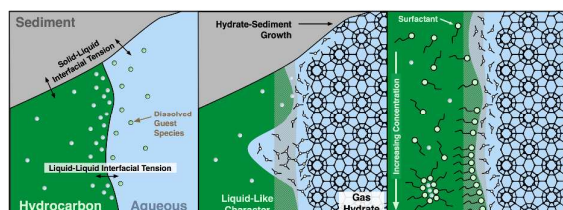

Figure 1. The different hydrate-fluid-solid interactions that play critical roles in all energy applications of hydrate research, including methane production from naturally occurring hydrate reservoirs (left, middle), hydrate growth during hydrocarbon transmission (middle, right), and technological applications including gas storage (not shown).

In conventional energy systems, hydrate particles may interact with liquid or gaseous hydrocarbon phases, liquid water, or the stainless steel pipeline wall. As such, the hydrate-specific interfaces of interest are highlighted in Figures 1 and 2: hydrate-gas, hydrate-oil, hydrate-water, and hydrate-steel.
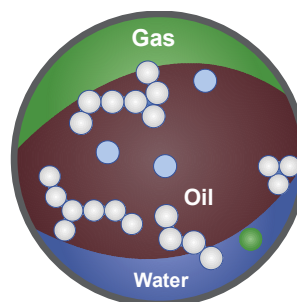

Figure 2. Conceptual schematic of multiphase flowline, where hydrate particles and aggregates (white solid) may flow in gas, oil, or water phases, and may deposit on the flowline.

In the past two decades, hydrate research has undergone a marked shift toward probing the interface, in an effort to gain better predictive control of how hydrate solids may behave in both natural and conventional energy systems. This article reviews the significant insights generated over the past two decades in understanding the hydrate interface, and highlights missing pieces of knowledge in the community.

Interfacial Thermodynamics

The free energy of the interface may be described by introducing an interfacial tension per unit area, to replace the pressure contribution in the Gibbs-Duhem equation:[23]

$$dG^\sigma = S^\sigma dT + A d\gamma^\sigma + \sum_j n_j^\sigma d\mu_j$$

(1)

where G^σ, S^σ, γ^σ and n_j^σ are the free energy, entropy, interfacial tension, and number of molecules at the interface, respectively, T is the system temperature, A represents the area of the interface, and μ_j is the chemical potential of molecules at the interface. Note that, in the free energy definition for interfaces, the differential volume and pressure terms have been replaced by a differential interfacial area and interfacial tension; this translation provides a context through which to interpret the physical contribution of interfacial tension in two-dimensional systems.

The chemical potential contribution may be neglected following Gibbs' formalism of the two-dimensional dividing surface, which occupies no volume. While this assumption is useful for simplifying calculations, it does not capture the gradient in continuous phase properties, such as density, when approaching the interface.[23] That is, there exists a density gradient from the interface into the continuous phase, resulting in an equilibrium super-saturation of each component in the region of the interface. This behaviour provides the physical basis behind the industrial heuristic[1] of hydrate nucleation[24] at the interface; methane and water are readily available, increasing the probability[25, 26] of stabilising the early hydrate cages.[27, 28]

Interfacial super-saturation is important to the practical application of inhibiting hydrates in the flowline, as the addition of polar hydrate thermodynamic inhibitors – including methanol[29] and salt ions[30] – may increase the equilibrium solubility of light hydrocarbons in the aqueous phase.[31] This behaviour also illuminates a risk when using cyclopentane as an ambient-pressure sII guest molecule, where severely reduced water solubility[32] limits both nucleation probability and growth rate.[33] In addition, the mixture of cyclopentane with liquid hydrocarbons (e.g. paraffin oil) has been reported to decrease the maximum hydrate stability temperature at 1 bar.[34] Limited reports have highlighted a potentially attractive sII hydrate-forming system, where cyclopentane is mixed with methane,[35] hydrogen or carbon dioxide[36] to reduce the required hydrate stability conditions. Alternatively, some refrigerants (e.g. R134a[37]) are attractive low-pressure hydrate formers, with high equilibrium solubility in the aqueous phase.[38] The initial growth of hydrate at the water-hydrocarbon interface is limited by this region of super-saturation, with the film thickness reported between 5 and 100 μm for methane hydrate.[39, 40] In the limit of a water-in-oil microemulsion, some studies have observed that interfacial metastability can require a stronger driving force for hydrate nucleation.[41]

After hydrate formation, the resultant hydrate crystal may exhibit an aqueous quasi-liquid layer (QLL) [42] at the hydrate-hydrocarbon interface. The layer thickness may range from nm[43] to μm,[33] and functions to decrease the global free energy in the system.[44] As the temperature decreases from 0 to 20 K below the solid melting temperature, the thickness of the liquid-like layer will decrease and ultimately disappear.[43] Similar layers have been confirmed for metals[45] and ice[46] near the melting temperature, but have only been inferred from indirect evidence for hydrate systems.[47] However, this common interfacial behaviour provides a microscopic basis with which to contextualise the "cold flow" operating approach for hydrate slurries,[48] where the capillary aggregation potential between hydrate particles is minimized deep inside the hydrate stability zone.

Hydrate Nucleation and Crystal Growth

The major hydrate nucleation and growth processes occur at the gas-liquid-solid interface. Hence, in order to control hydrate formation and decomposition in all different energy applications requires advanced understanding and control of hydrate interfacial processes. Figure 3 illustrates the conceptual model that has been proposed for hydrate nucleation.[1] The formation of labile water clusters (5^{12}, $5^{12}6^2$, $5^{12}6^4$) that are comprised of the known hydrate cages found within the sI and sII structures are integral to this nucleation model. These labile clusters can then interact/agglomerate to form critical crystal nuclei that can grow to hydrate unit cells.
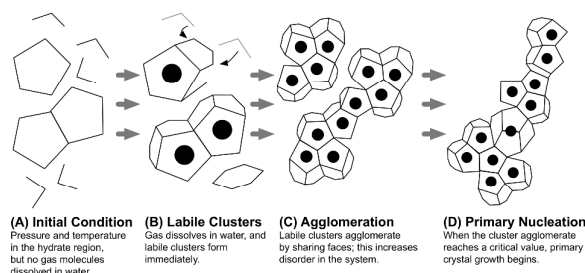

(A) Initial Condition Pressure and temperature in the hydrate region, but no gas molecules dissolved in water

(B) Labile Clusters Gas dissolves in water, and labile clusters form immediately.

(C) Agglomeration Labile clusters agglomerate by sharing faces; this increases disorder in the system.

(D) Primary Nucleation When the cluster agglomerate reaches a critical value, primary crystal growth begins.

Figure 3. Conceptual model of hydrate nucleation at the liquid-gas interface. This image is reproduced with permission from Sloan and Koh.[1]

Although first suggested by Sloan and co-workers in the mid-1990's,[49, 50] more recent molecular simulations of hydrate nucleation have revealed features/elements that are consistent with the labile cluster hypothesis.[24] Specifically, microsecond-scale simulations show that key hydrate cages are formed as guest molecules interact with the faces/surfaces of partial hydrate water cages during the nucleation process (Figure 4). In addition to the common 5^{12}, $5^{12}6^2$, and $5^{12}6^4$ water cages, other exotic water cages ($5^{12}6^3$) are formed. These cages connect together to form different sI/sII type-

motifs/clusters (Figure 5), which provide the building blocks to hydrate crystal growth.

After the hydrate nucleation events, crystal growth progresses from the critical crystal nucleus. Similar to nucleation mechanics, crystal growth of hydrates occurs at the gas-liquid-solid interfaces. The conceptual picture for hydrate crystal growth is illustrated in Figure 6, which has elements borrowed from general crystal growth mechanics. A hydrate/water cluster interacts with the solid hydrate crystal surface (i), then either attaches to the surface (ii), or diffuses across the surface (iii), and attaches to the hydrate step (iv) or kink sites (v). Water molecules are expelled as the water clusters attach and are incorporated into the hydrate crystal structure.

The nucleation and crystal growth conceptual models help to illustrate the requirement to control the various interfaces in order to promote or inhibit hydrate formation. Interference of these processes can therefore occur via surfactant/chemical adsorption at the hydrate crystal nuclei surfaces and crystal growth planes, as discussed below.

Figure 5. Molecular simulations reveal motifs of the hydrate crystal structure, which comprise common and more exotic hydrate water cages. Pink cages: 5^{12}; Red cages: $5^{12}6^2$; Brown (linking) cages: $5^{12}6^3$; Blue cages: $5^{12}6^4$; Yellow shading: sI motif; Blue shading: sII motif. This image is reproduced with permission from Walsh et al.[24]

Molecular experimental studies of the hydrate nucleation and crystal growth processes are challenging due to the small dimensions at which these pathways take place (i.e. nanometer-scale), as well as the short timescales (microseconds for nucleation), and stochastic nature of hydrate formation.[18, 51] Experimental studies of crystal growth processes are more accessible given the larger dimensions and longer timescales (as well as being less stochastic than nucleation, which depends on rare events), though molecular measurements are still challenging.
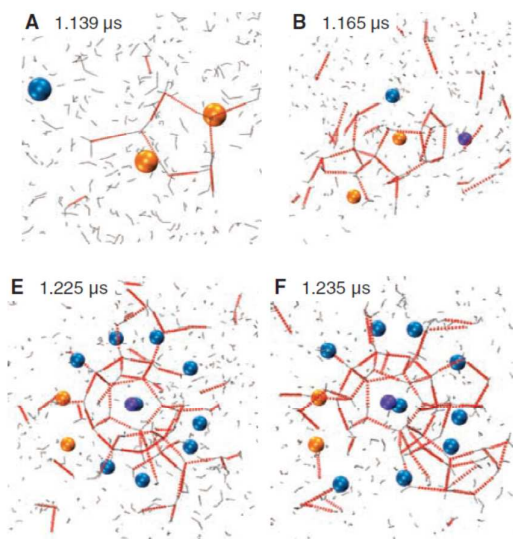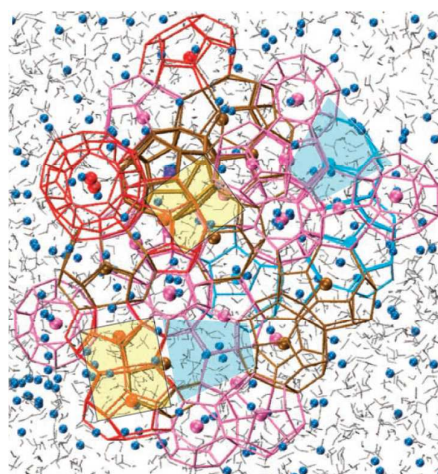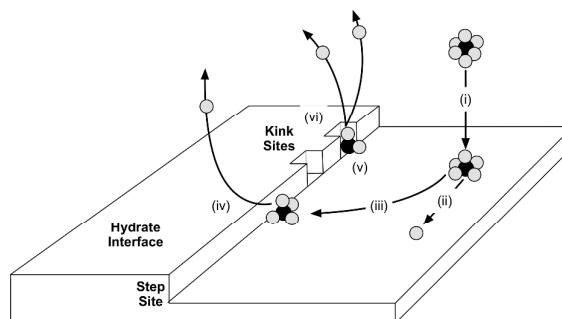

Figure 4. Microsecond-scale molecular simulations of hydrate nucleation show hydrate cages are formed as guest molecules interact with the surfaces/faces of the partial water cages. This image is reproduced with permission from Walsh et al.[24]

Figure 6. Conceptual model of hydrate crystal growth, redrawn with permission from Sloan and Koh,[18] where a guest molecule (black circles) surrounded by a transient water cluster (grey circles) adsorbs to the growing hydrate interface; as the guest molecule is incorporated in the growing cage network, water molecules can diffuse back into the fluid phase.

Several studies have been performed to examine hydrate single crystal formation and the visual observation of the evolution of crystal planes. The structural evolution of hydrate crystal growth has been performed via Raman spectroscopy and solid-state NMR spectroscopy, as well as x-ray and neutron diffraction. Guest molecules incorporated into hydrate cages within the hydrate crystal can be detected by Raman and NMR, while crystal growth phases are detected with x-ray and neutron measurements.[1]

Hydrate Interfacial Tension

Due to the typically large surface area involved in hydrate-rich systems, interfacial tension accounts for a substantial portion of the total free energy.[52, 53] While simple experimental techniques, such as droplet volume or pendant drop, may be used to probe the interfacial tension between two fluids,[54] such techniques are inappropriate to probe solid-fluid interfaces. One strategy has exploited sessile drop contact angle measurements, which may be used to estimate solid-fluid interfacial tension.[55] Asserson et al.[56] applied this technique to estimate the wetting angle of Freon hydrate in brine at 29°, but the distributed nature of hydrate film growth hinders the repeatability of this measurement technique.

Micromechanical force (MMF) measurements between hydrate particles,[57] which are discussed further below, have demonstrated one methodology to estimate hydrate-fluid interfacial tension. Using cyclopentane hydrate, analysis[58] of cohesive force measurements suggest a hydrate-cyclopentane interfacial tension of 47 ± 5 mN/m, which compares well with an approximation proposed by Kwok and Neumann[59, 60] that yielded 45 mN/m using the wetting angle data referenced above.[56]. As a comparison, the water-cyclopentane interfacial tension is approximately 51 mN/m.[61] This comparison suggests that the hydrate surface, when exposed to a liquid hydrocarbon, may be similarly energetic to that of water; Young's equation provides a context through which to estimate the hydrate-water interfacial tension (< 0.5 mN/m) with the above values. This hydrate-water interfacial value is two orders of magnitude below literature reports of gas hydrate-water interfacial tension, which are distributed without trend between 14 ± 3 and 45 ± 1 mN/m for methane, ethane, or propane hydrates.[62-64] These later estimations were indirectly derived from porous media measurements, where large variations in pore size and wetting angle may give rise to discrepancies. The measurement or estimation of hydrate-fluid interfacial tension remains a primary knowledge gap, as this property controls the adsorption and packing of surfactants at the hydrate crystal surface.

An example of the temperature dependence of hydrate cohesion is shown in Figure 7 from MMF data reported by Aman et al.[33] The cohesive forces in Figure 7 were reported with the logarithm of the inverse hydrate subcooling, or the difference between the hydrate equilibrium temperature (T_{eq}) and system temperature (T). The absicssa was chosen based on disscussion from Nenow et al.,[44] who demonstrated from the first principles derivation by Dzyaloshinskii et al.[42] that a crystalline QLL height should vary linearly with the logarithm of the inverse hydrate subcooling. The direct quantification of the hydrate QLL remains an outstanding experimental variable. However, the data in Figure 7 represent the closest indirect confirmation of the hydrate QLL to date.
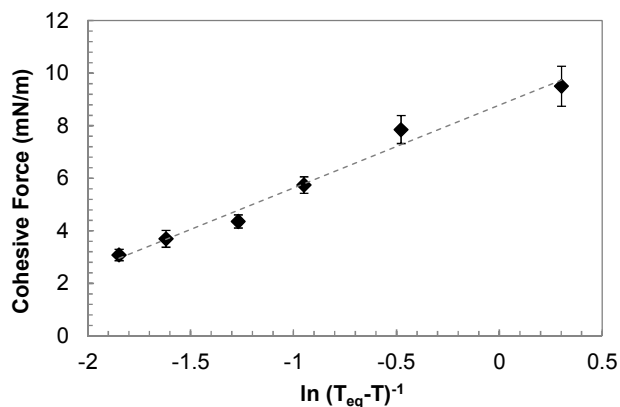

Figure 7. Hydrate cohesive force reported by, and reproduced with permission from Aman et al.[33] as a function of temperature. Error bounds represent a 95% confidence interval on the measured cohesive force; the dashed line is provided to guide the eye.

Surfactant Adsorption

The form of equation (1) illustrates the importance of hydrate-fluid interfacial tension in controlling the free energy of the system. In conventional energy systems, surfactants from both natural (oil) and synthetic (injection) sources are readily available and may interact with accessible high-energy interfaces. Furthermore, in the case of unconventional energy systems, the presence of biosurfactants may play some role in hydrate evolution during the formation of natural hydrate deposits and/or the hydrate dissolution process, which can lead to natural release of methane into the neighboring atmosphere in oceanic and permafrost locations.[65] When presented with a high-energy, hydrophilic-hydrophobic interface, nearby ionic and nonionic surfactants may migrate and adsorb to this interface. There exists a substantial knowledge gap in understanding why surfactants exhibit unique affinity for the hydrate-hydrocarbon boundary. As a consequence, the current generation of studies has focused on proposing mechanisms for surfactant adsorption. In the case that interfacial tension can be measured as a function of surfactant concentration,[66] equation (1) may be re-arranged[67] at equilibrium to directly solve for the surfactant packing;[68, 69] the resultant quantity may take units of $Å^2$/molecule.

The use of the Gibbs-Duhem equation represents a repeatable method to quantify surfactant adsorption, but requires explicit knowledge of interfacial tension. To date, only MMF measurements have been used to rank the adsorption of surfactants at the hydrate-hydrocarbon boundary,[58] through the indirect solution of hydrate-hydrocarbon interfacial tension; those results suggested differentiable packing between a simple sulfonic acid and a complex carboxylic acid in the hydrocarbon phase, where the surfactants adsorbed to the hydrate surface with a maximum packing of 4.7 ± 0.5 and 27 ± 2.5 $Å^2$/molecule, respectively. Further studies are required to establish the limits of this MMF technique, but the measurement does provide an attractive means to quantify the equilibrium of multiple surfactants as an interfacial-

selective alternative to the macroscopic methods discussed below.

Most mechanistic studies have used well-studied hydrate-active chemistries, such as sodium dodecyl sulphate (SDS). Lo et al.[70] proposed that SDS may primarily adsorb to hydrate surfaces through hydrogen bonding, which qualitatively agrees with the differential adsorption estimates from MMF measurements described above.[58] Spectroscopic evidence of changes to the water structuring during SDS adsorption was presented by Lo et al.,[71] who proposed that the SDS hydrophobic group may interact directly with the hydrate surface at low concentrations.[72] The basic theme of hydrogen-bonded hydrophilic groups agrees with early molecular dynamics simulations from Carver et al.,[73] who suggested the availability of pendant hydrogen molecules on the hydrate surface acted as a control to surfactant adsorption spacing. While SDS may be commonly considered as a "model" hydrate-active surfactant, visual observations from Aman et al.[74] demonstrate that the surfactant encourages dendritic hydrate growth at moderate concentrations; further investigation is required with alternative nonionic surfactants (which have been confirmed to not affect hydrate morphology), prior to the acceptance of a fundamental adsorption mechanism.

Limited evidence has been presented to further suggest that kinetic hydrate inhibitors (KHIs), such as polyvinylcaprolactam (PVCap), may similarly adsorb to hydrate surfaces and reduce hydrate-hydrocarbon interfacial tension,[75] with a dependence on KHI solubility in the continuous phase.[76] Wu et al.[77] quantified a reduction in hydrate cohesive force – which may correspond to a decrease in hydrate-hydrocarbon interfacial tension[58] – when PVCap was present; further observation of the system suggested that PVCap decreased the rate of hydrate growth, as also observed in bulk crystal growth studies.[1] Together, this evidence suggests the potential for hybridized low-dosage hydrate inhibitors (LDHIs),[78] with the capability to retard hydrate growth rate and simultaneously decrease hydrate interfacial tension with fully-converted particles.

Crystal Growth

After hydrate nucleation at the water-hydrocarbon interface, the resultant growth rate and crystal morphology depends on both the subcooling from hydrate equilibrium and presence of surfactants in either phase. In quiescent systems, high subcooling may increase the hydrate film growth rate[79] and enable local transport resistances due to the exothermic heat of formation.[1] Rapid growth may result in the formation of dendrites[80] with smaller crystal surfaces[81] at the advancing crystal interface, to maximise crystal surface area-to-volume and more effectively release heat.

While the crystal growth rate has not been shown to change substantially with ion concentration in the aqueous phase,[82]

multiple studies have confirmed the effect of surfactants on hydrate growth rate. Kumar et al.[83] observed that SDS below 4000 ppm may enhance the crystal growth rate and decrease hydrate induction time; a similar observation was made by Yoslim et al.[84] for surfactants with sulphate groups. In the MMF study of dodecyl benzene sulphonic acid (DDBSA), Aman et al.[58] observed no change in hydrate-hydrocarbon interfacial tension below approximately 10^{-4} mol/l. Crystal growth measurements based on visual observation (Figure 8) demonstrated a substantial reduction in cyclopentane hydrate growth rate below this adsorption threshold.

This result critically demonstrates that DDBSA decreased the hydrate growth rate by approximately a factor of four, at concentrations below which it measurably affected the hydrate-hydrocarbon interfacial tension. At higher concentration, DDBSA has been suggested to reduce the hydrate-cyclopentane interfacial tension to a minimal value (< 2 mN/m);[58] under this condition, Aman et al.[33] observed an increase in cyclopentane hydrate growth by more than two orders of magnitude. Similar crystal growth consequences were noted by Norland et al.[85] for select ammonium salts.
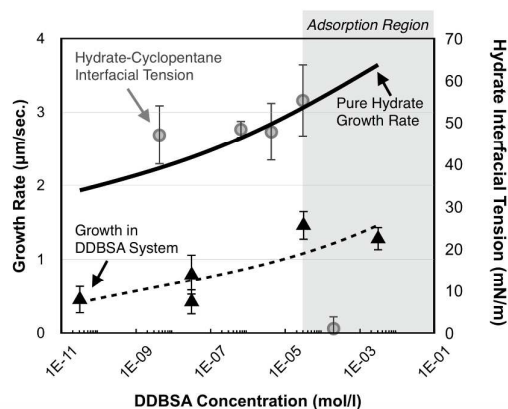

Figure 8. Cyclopentane hydrate film growth rate with (black triangles) and without[33] (solid curve) DDBSA in the continuous cyclopentane phase, with error bounds representing one standard deviation of growth rate measurements; the dashed line is provided to guide the eye. Hydrate-cyclopentane interfacial tension data (circles) correspond to the right-hand ordinate, with error bounds at 95% confidence; the data indicate DDBSA strongly adsorbs to the hydrate surface above approximately 10^{-4} mol/l. Reproduced with permission from Aman et al.[58]

Application in Conventional Energy Systems

Hydrates are a common engineering challenge in hydrocarbon transport flowlines, typically requiring significant capital and operating expenditure to manage.[86] In severe cases, hydrate growth may result in complete blockage of the flowline, according to a four-step mechanism proposed by Turner et al.[87] in collaboration with J. Abrahamson (Figure 9): (i) water emulsification in the liquid hydrocarbon phase; (ii) hydrate nucleation and growth at the water-hydrocarbon interface; (iii)

particle aggregation; and (iv) blockage formation from aggregate jamming.[88, 89]

For liquid hydrocarbon phases with high dynamic viscosity and/or a large volume of natural surfactants,[90] the volume fraction of dispersed water (watercut) may reach up to 90%.[91] With increasing watercut, all systems will eventually reach a condition under which the oil-in-water and water-in-oil dispersed phase energies equilibrate; at this point, the system will "invert" with water as the continuous phase.[92] As the water-in-oil emulsion is generally a precursor to hydrate formation, a semi-empirical model from Boxall et al.[93] may typically be applied:

$$D_{\text{Particle}}^{(\text{inertial})} = C_1 D_{\text{Flow}} \left(\frac{\rho v^2 D_{\text{Flow}}}{\gamma} \right)^{k_1} \tag{1}$$

$$D_{\text{Particle}}^{(\text{viscous})} = C_2 D_{\text{Flow}} \left(\frac{\rho v^2 D_{\text{Flow}}}{\gamma} \right)^{k_2} \left(\frac{\rho v D_{\text{Flow}}}{\mu} \right)^{k_3} \tag{2}$$

where $D_{\text{particle}}^{(\text{inertial})}$ and $D_{\text{particle}}^{(\text{viscous})}$ are the mean particle diameters produced by the inertial and viscous modes, respectively, D_{Flow} is the cross-sectional diameter of the flowpath, v is the mixing velocity, γ is the water-oil interfacial tension, and ρ and μ are the density and viscosity of the bulk phase, respectively.

The model builds upon the pioneering work of Kolmogorov[94] and Hinze,[95] where droplet size is determined by a balance of shear stress from the continuous phase and interfacial restorative force for both viscous and inertial sub-regimes.[96, 97]

In practice, the high shear rates and hydrocarbon phase viscosities encountered in most flowlines will generate water droplet diameters below 100 μm. The range of hydrate film thicknesses presented above (5-100 μm) suggest that most water droplets will fully convert to hydrate upon nucleation. In the limiting case of large droplets, a hydrate shell[98] may enclose the water droplet, with further conversion limited by mass transport across the hydrate crystallites;[99] static mixing systems may also be used in practice to generate smaller droplet sizes to facilitate complete conversion to hydrate particles.[100]

The resultant hydrate particles may aggregate to form a fractal structure,[101] based on a similar force balance between continuous phase shear stress and interparticle cohesive force.[102-104] In hydrate systems, Sinquin et al.[105] have demonstrated the use of Mills model[106] to account for increases in slurry viscosity:

$$\mu_{relative} = \frac{1 - \Phi_{eff}}{\left(1 - \frac{\Phi_{eff}}{\Phi_{max}} \right)^2} \tag{3}$$

where Φ_{eff} and Φ_{max} respectively describe the effective and maximum allowable particle volume fractions, and $\mu_{relative}$ is the relative viscosity of the hydrate-laden slurry.

While alternative slurry viscosity models are available,[107] limited data are available to describe the rheology of model particle-in-hydrocarbon[108] or real hydrate-in-oil[109, 110] systems.

Particles above the micron lengthscale are not highly susceptible to dispersion forces from surface charge, resulting in three potential mechanisms to enable cohesive force between two particles:[111] (i) solid-solid cohesion, where force is proportional to the product of particle-fluid interfacial tension and area generated by cohesive failure;[112, 113] (ii) capillary liquid bridge cohesion,[114, 115] where force depends on the bridge-fluid interfacial tension and bridge-particle wetting angle;[116, 117] and (iii) sintering or growth between the particles, where force is proportional to the product of the solid tensile strength and minimum sintered area.[118]

Dieker et al.[119] suggested that cohesion between cyclopentane hydrate shells (containing a water core) followed a capillary bridge dependence, where the hydrate surface may exhibit a liquid-like interfacial layer as discussed above. Taylor et al.[120] observed tetrahydrofuran (THF) cohesive forces that were both temperature- and time-dependent, which may be the result of rapid particle sintering[121] due to the miscibility of THF in the aqueous phase. Lee et al.[122] have suggested that fully-converted particles may follow a solid-solid cohesive mechanism in the absence of liquid water, which agrees with high preload force measurements from Maeda et al.[123] If a liquid bridge is present, from either an interfacial liquid-like layer or unconverted water contacting the particle, Aman et al.[33] proposed a sintering mechanism to govern hydrate cohesion at long timescales. Due to the transport limitations commonly encountered with hydrate growth in a continuous hydrocarbon phase,[124] the initial growth of hydrate may be accompanied by an unconverted water volume that enables a high capillary bridge force between the particles; this sequence may explain the initial peak in slurry viscosity observed for hydrate-in-hydrocarbon systems.[34, 110, 125]
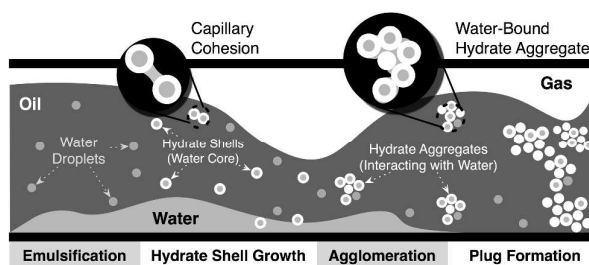

Figure 9. Conceptual mechanism of hydrate blockage formation in hydrocarbon transport flowlines, based on the discussion from Turner et al.[87] and reproduced with permission from Aman et al.[126]

Both solid-solid and capillary bridge particle cohesion depend critically on hydrate-hydrocarbon interfacial tension,[111] which is highly sensitive to surfactants in the continuous phase. For these reasons, the adsorption of natural and synthetic

surfactants to the hydrate interface is a critical step in assessing the aggregation potential between hydrate particles.

Through the conceptual mechanism in Figure 9, hydrate blockages may be identified by increases in apparent slurry viscosity above a value of 100.[127] In reality, the physical blockage is defined by a decrease in fluid velocity toward zero, where the increasing pressure drop reduces the energy available to maintain fluid momentum.[128, 129] While particle aggregation plays an undeniably important role in decreasing fluid velocity,[90] the deposition of hydrate particles on the pipeline wall provides a complementary effect.[130, 131] Recent field-scale studies from Lachance et al.[132] have highlighted the importance of particle deposition, but there is currently a dearth of experimental data with which to fundamentally describe build-up rate at the pipe wall in oil-continuous systems. Through bench-top MMF studies, Nicholas et al.[133] have reported strong adhesion forces when the particles were allowed to sinter with steel surfaces; Aspenes et al.[134] determined that naphthenic acids (discussed further below) may provide one solution to reduce or eliminate wall adhesion forces. While these data provide valuable insight, there is missing data at the mesoscopic length-scale on the population balance of hydrate particles throughout the oil phase,[135] similar to what was developed by Joshi et al.[136] for water-continuous systems where aggregation forces are minimised.[137]

Chemical Inhibitors

Over the past ten years, the development and application of low-dosage hydrate inhibitors (LDHIs) has provided new pathways for hydrate management in complex engineering systems. Two classes of LDHIs have been developed to date: hydrate anti-agglomerants (AAs) and kinetic hydrate inhibitors (KHIs).[78] Sloan et al.[138] provide an example of KHI structures, which utilise variants of vinylic polymers with either amine or imide groups; these are thought to adsorb to partially-formed hydrate cages, disrupting the formation of a critical nucleus. Both PVCap and polyvinylpyrrolidone (PVP) are common KHI structures, which delay the onset of macroscopic hydrate growth in systems within the equilibrium region. KHIs represent a promising technological change, where multiphase systems may be allowed to cool into the hydrate stability region without forming hydrate (i.e. KHIs will cause long time delays before hydrate nucleation/growth occurs). The development and validation of KHIs has traditionally been performed through a rocking cell,[139] while the adaptation of an automated lag-time apparatus (ALTA)[26, 140] for hydrate nucleation has demonstrated accuracy and a stronger quantitative ranking potential for KHI chemical development.[25] Some studies have deployed cyclopentane as a sII hydrate former for KHI ranking, but recent evidence has suggested this may not be appropriate; Song et al.[141] reported PVP and PVCap did not affect the water adhesion energy to hydrate surfaces, while Dirdal et al.[76] were unable to differentiate KHI

performance in cyclopentane systems. As the guest species interfacial super-saturation depends on equilibrium solubility, gas hydrate species (e.g. methane) may be required for future KHI ranking. This experimental scheme is particularly important to ensure any morphological growth features induced by KHI addition[142] remain unaffected by mass and heat transport limitations.

Hydrate anti-agglomerants (AAs) function whereby surfactants may prevent hydrate particle aggregation and enable a stabilised hydrate-in-oil slurry. Most AAs are based on quaternary ammonium salts,[143] where the ionic surfactant may be associated with a variety of hydrophobic groups. AAs have historically been represented in well-characterised laboratory studies by sorbitan-class surfactants (e.g. Span20 to Span80).[144] Recently, Span80 has been associated with dendritic growth on the hydrate surface, indicating the chemical may prevent particle aggregation through an alternative pathway to ionic surfactants.[74] AAs have been shown to increase in effectiveness with an alcoholic co-surfactant (e.g. methanol[145]), and with the saline content in water.[146] The proprietary nature of AA chemistry has precluded academic discussion of chemical functionality over the past decade, while industrial research has demonstrated significant advances in the ability to minimise emulsion stability.[147] That is, emulsions must be destabilised after leaving the flowline with either high temperature[148] or chemically-tuned demulsifiers.[149] In recent years, one new AA structure (cocamidopropyl dimethylamine) has received attention for its ability to function in the water-continuous phase,[150] which may provide a pathway beyond the expected 50 vol.% watercut limitation for previous-generation AAs.[151]

Hydrate-Active Surfactants

In addition to the synthetic surfactants discussed above, crude oils provide a rich environment of natural surfactants that duly interact with high-energy interfaces.[152] Sjöblom et al.[90] highlighted the performance of unique crude oils that naturally suspend hydrate particles in crude oil; this behaviour was attributed to a distribution of natural surfactants that supressed capillary cohesion by reducing water-oil interfacial tension and generating oil-wet hydrate particles. An example of this behaviour is shown in the bottom two panels of Figure 10; when one such crude oil is injected in the continuous phase, a high (> 2 mN/m) preload force may be applied between a *water* droplet and cyclopentane hydrate particle. When the same experiment is performed in liquid cyclopentane, the water droplet immediately wets the hydrate particle surface (top two panels of Figure 10). This simple experiment demonstrates that this crude oil readily generates a hydrophobic hydrate surface, which does not interact with liquid water.
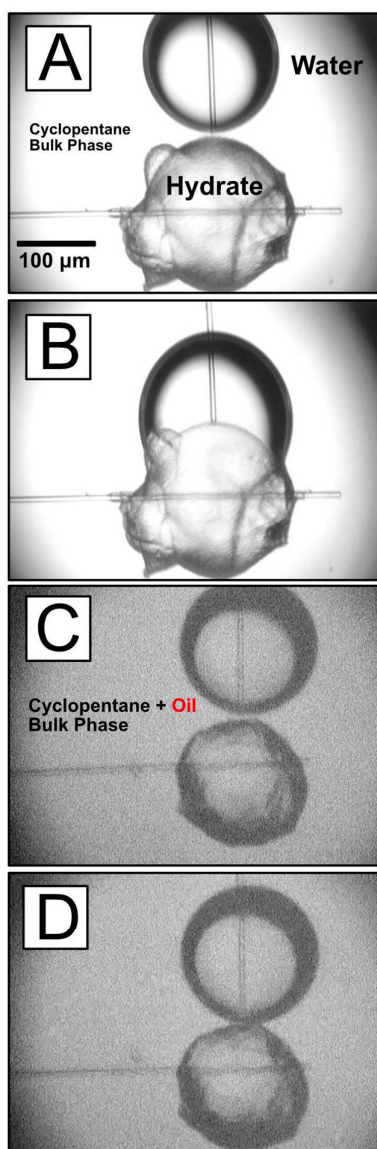
Figure 10. Microscopic images of a deionised water droplet (top particle) interacting with cyclopentane hydrate (bottom particle): (A) prior to contact in cyclopentane; (B) immediately after contact in cyclopentane; (C) prior to contact in cyclopentane + crude oil; and (D) after a preload force is applied in cyclopentane + crude oil.

Borgund et al.[153, 154] qualitatively observed that oils may naturally suspend hydrate particles when the total acid number (TAN) was larger than the total base number (TBN). Spectral analysis by Clemente et al.[155, 156] suggested that naturally-occurring amphiphilic compounds in crude oil may contain large fractions of carboxylic acid. Ester carbonyl functional groups were suggested to enable hydrophobic hydrate surfaces by Erstad et al.,[157] after extracting and studying an array of naphthenic acid fractions from multiple oils.[158] Barth et al.[159] and Genov et al.[160] linked the relative fraction of these moieties to the degree of reservoir biodegradation;[161] Gasson et al.[162] further suggested that oils with a large fraction of branched short carbon chains exhibited

similar dispersion stability. Fafet et al.[163] suggested that biodegraded naphthenic acids may contain multiple ring structures, where Barrow et al.[164] identified carbon number ranges of 15-35 with hydrogen deficiencies up to 26; similar results were observed by Headley et al.[165]

ARN tetra-acids[166, 167] may provide an attractive candidate to explain emulsion and dispersion stability in crude oils.[168] The latter may contain 4-6 polyaromatic acids within the structure.[169] While ARN acids have been shown to affect surface wettability,[170] there has been limited success in quantifying the effect of these compounds on hydrate cohesive force.[171] Studies have instead focused on the existence of a polyaromatic hydrophilic moiety to promote surfactant adsorption.[172, 173] Aman et al.[174] identified a strong (> 90%) reduction in hydrate cohesive force when pyreneacetic acid was present in the continuous phase; additional experiments are required to identify whether these polyaromatic structures are related to the resin or asphaltene oil fractions.[148] Recent studies[154] have further explored the use of biosurfactants, with signature amine moieties,[175]and may provide a new pathway to developing biocompatible hydrate-active surfactants. A functional representation for AAs, KHIs, and natural surfactants are shown in Table 1. Particularly in the case of AAs and natural oil surfactants, an increase in the salinity of the aqueous phase, which can reach saturation limits in some formation water (particularly as hydrates are formed, thereby concentrating the salt within the unconverted remaining water), may enable stronger surfactant adsorption to the hydrate-oil interface.

Table 1. Example of low-dosage hydrate inhibitor chemical structures, which may prevent hydrate particle aggregation and/or growth by adsorbing to the crystal surface.

Name	Example Structure	Application
Anti-Agglomerant (ionic surfactant)		Weakens hydrate aggregation force, enabling flowable slurry[78, 144]
Kinetic Hydrate Inhibitor (polymer)		Supresses crystal growth for long periods, enabling extended shut-in of flowlines[49, 50]
Natural Oil Surfactant (non-ionic)		May adsorb to hydrate particles, preventing aggregation[90]

Improving Measurements of Hydrate Dispersion Stability

In the past decade, three experimental methods have delivered a step change in understanding and testing hydrate interfacial behaviour: the MMF apparatus, as discussed above; hydrate dispersion stability measurements using differential scanning calorimetry (DSC);[176] and a high-pressure sapphire autoclave that delivers simultaneous information on slurry formation and wall deposition/film growth.[177] The latter method follows the same procedure as previously established for autoclave measurements.[178] The DSC method is a relatively new development,[179] which was originally used to study hydrate agglomeration in drilling muds.[180] In this method, hydrate is formed and dissociated from a water-in-oil emulsion under high pressure over 3-5 cooling-heating cycles. When the hydrate dissociates due to heating, an unstable dispersion will allow droplet coalescence; in the next hydrate formation step, less hydrate will form due to a limited thickness of the initial shell (as discussed above). In this way, the DSC may be used to track the destabilisation of hydrate-in-oil dispersions with hydrate formation, the concept of which is demonstrated in Figure 11.[181] A similar effect of hydrate dissociation was observed by Chen et al.[41] using a sapphire cell similar to the design referenced above.
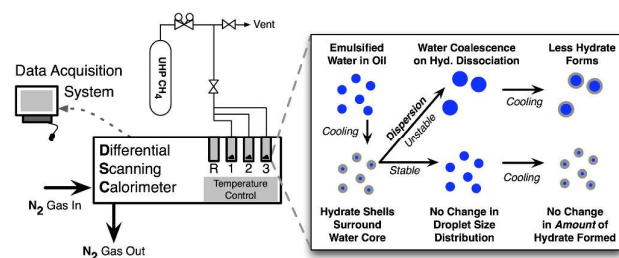

Figure 11. Schematic of multi-cell DSC, reproduced with permission, from Aman et al.,[126] where hydrate-in-oil suspensions are generated by cooling water-in-oil emulsions under high pressure. If the hydrate suspension remains stable, no change is observed in the total amount of hydrate conversion measured over repeated heating and cooling cycles.

Aman et al.[126] have recently demonstrated the use of DSC measurements to introduce surfactants (e.g. quaternary ammonium salts) in the oil phase, and quantify changes to the rate of destabilisation as a function of surfactant concentration (*cf*. refs.[90,180]). Uniquely, these recent studies have found that the surfactant concentration required to stabilise hydrate-in-oil dispersions within the DSC is different from the strong adsorption region to the water-oil interface (quantified via the pendant drop method); this suggests that droplet coalescence in the DSC may be determined by the concentration and type of surfactants that are near/adsorbed to the *hydrate* interface prior to dissociation.

The current generation of hydrate aggregation studies typically involves large-scale flowloops, where hydrate aggregate diameter[182] and fractal dimension[101] are quantified through microscopic or reflectance[183] methods that can be in-line on the flowloop. In the case that such measurements are not paired with rigorous population balance models,[184] interfacial-level quantification (e.g. cohesive force) may be only estimated with substantial uncertainty. Instead, the new bench-top MMF, DSC and autoclave technologies described above may be used to deliver the fundamental properties required for direct interpretation of macroscopic (flowloop-scale) systems.

Future Directions

The interface plays a critical role in determining the macroscopic behaviour of hydrate systems. As the community moves beyond thermodynamics to kinetics studies and control, and beyond volumetric measurements, there are three frontiers at which the interfacial phenomena contribute to the management of hydrates in energy systems:

- Hydrate nucleation and film growth is determined by the super-saturation across the interface, which is a function of both the thermodynamic conditions and the equilibrium cross-solubility of the species.
- Hydrate particle aggregation is a function of both water-oil and hydrate-oil interfacial tension, where there is insufficient and inconsistent data available in literature to describe the latter quantities.
- Surfactant adsorption to the hydrate-oil interface represents a frontier in technology development, where both the MMF and DSC have shown promising potential as tools to address this problem.
- Hydrate adhesion to the wall, which has been recently identified[132] as a critical mechanism to blockage in flowlines; preliminary studies have demonstrated an ability to reduce or eliminate wall adhesion through chemical[185] or physical[186] modifications to the wall. To date, these technologies have not been up-scaled to high-pressure flowing systems, but provide a promising pathway for future development.

The current understanding of surfactant interaction with hydrate – through both KHIs and AAs – suggests an overlap in functional behaviour, where adsorbed surfactant species may duly inhibit hydrate crystal growth, as well as inter-particle cohesion. While significant development to date has focused on variations of ionic surfactants, closer analysis of hydrate-philic natural surfactants suggests that nonionic hydrophilic moieties (e.g. carboxylic acid) in combination with polyaromatic hydrophobic groups may provide a pathway toward the development of natural AAs.

Furthermore, hydrate molecular and macroscopic control at the gas-liquid-solid interface should also consider the chemical formulation rules that are well-established in the surfactant field, and that was proposed initially for hydrate control by Zerpa et al.[152] Interfacial modelling (e.g. DFT and reactive molecular dynamics simulations) and measurement

techniques (e.g. atomic force microscopy, micromodels/microfluidics, small angle neutron scattering), as well as mechanistic understanding traditionally adopted for the colloid and emulsion fields should be also considered, adapted and applied for hydrate interfacial studies. Adaptations of this richer/more mature knowledge base to hydrate understanding can likely lead to the breakthrough advances required in controlling/modelling the hydrate interfacial formation/dissociation processes for all energy applications.

Acknowledgements

References

1. E. D. Sloan and C. A. Koh, *Clathrate Hydrates of Natural Gases*, CRC Press, Taylor & Francis Group, Boca Raton, FL, Third Edition edn., 2007.
2. E. G. Hammerschmidt, *Industrial & Engineering Chemistry*, 1934, **26**, 851-855.
3. E. D. Sloan, C. A. Koh and A. K. Sum, *Natural Gas Hydrates in Flow Assurance*, Gulf Professional Publishing, Elsevier Inc., 2011.
4. Y. F. Makogon, *Gazov Prom-st*, 1965, **5**, 14-15.
5. K. A. Kvenvolden, *Annals of the New York Academy of Sciences*, 1994, **715**, 1-15.
6. E. D. Sloan, *Nature*, 2003, **426**, 353-363.
7. C. A. Koh, E. D. Sloan, A. K. Sum and D. T. Wu, *Annual Review of Chemical and Biomolecular Engineering*, 2011, **2**, 237-257.
8. H. Lee, J.-w. Lee, D. Y. Kim, J. Park, Y.-T. Seo, H. Zeng, I. L. Moudrakovski, C. I. Ratcliffe and J. A. Ripmeester, *Nature*, 2005, **434**, 743-746.
9. N. Kalogerakis, P. D. Dholabhai, P. Englezos and P. R. Bishnoi, *Chemical Engineering Science*, 1987, **42**, 2659-2666.
10. A. Vysniauskas and P. R. Bishnoi, *Chemical Engineering Science*, 1983, **38**, 1061-1072.
11. A. Vysniauskas and P. R. Bishnoi, *Journal*, 1985, **40**, 299-303.
12. P. Skovborg and P. Rasmussen, *Chemical Engineering Science*, 1994, **42**, 1131-1143.
13. E. D. Sloan, *Energy & Fuels*, 1998, **12**, 191-196.
14. Infochem, *Journal*, 2012.
15. A. L. Ballard and E. D. Sloan, *Fluid Phase Equilibria*, 2004, **218**, 15-31.
16. A. L. Ballard and E. D. Sloan, *Fluid Phase Equilibria*, 2004, **216**, 257-270.
17. M. Clennell, M. Hovland, J. Booth, P. Henry and W. Winters, *Journal of Geophysical Research*, 1999, **104**, 22985-23003.
18. C. A. Koh, A. K. Sum and E. D. Sloan, *Journal of Applied Physics*, 2009, **106**.
19. J. Dvorkin, J. Berryman and A. Nur, *Mechanics of Materials*, 1999, **31**, 461-469.
20. W. F. Waite, J. C. Santamarina, D. D. Cortes, B. Dugan, D. N. Espinoza, J. Germaine, J. Jang, J. Jung, T. Kneafsey, H. S. Shin, K. Soga, W. Winters and T. S. Yun, *Reviews of Geophysics*, 2009, **47**.
21. C. Ecker, J. Dvorkin and A. Nur, *Geophysics*, 1998, **63**, 1659-1669.
22. J. W. Jung and J. C. Santamarina, *Geochemistry Geophysics Geosystems*, 2011, **12**.
23. E. B. Naumann, *Chemical Reactor Design, Optimization, and Scaleup*, John Wiley & Sons, New Jersey, Second Edition edn., 2008.
24. M. R. Walsh, C. A. Koh, E. D. Sloan, A. K. Sum and D. T. Wu, *Science*, 2009, **326**, 1095-1098.
25. E. F. May, R. Wu, M. A. Kelland, Z. M. Aman, K. A. Kozielski, P. G. Hartley and N. Maeda, *Chemical Engineering Science*, 2014, **107**, 1-12.
26. R. Wu, K. A. Kozielski, P. G. Hartley, E. F. May, J. Boxall and N. Maeda, *AIChE Journal*, 2013, **In Press**.
27. B. C. Barnes, G. T. Beckham, D. T. Wu and A. K. Sum, *The Journal of Chemical Physics*, 2014, **140**, 164506.
28. B. C. Barnes, B. C. Knott, G. T. Beckham, D. T. Wu and A. K. Sum, *J. Phys. Chem. B*, 2014, **118**, 13236-13243.
29. K. Kinnari, J. Hundseid, X. Li and K. M. Askvik, *J. Chem. Eng. Data*, 2015, **60**, 437-446.
30. M. Kharrat, *The Journal of Chemical Thermodynamics*, 2003, **35**, 1489-1505.
31. L.-K. Wang, G.-J. Chen, G.-H. Han, X.-Q. Guo and T.-M. Guo, *Fluid Phase Equilibria*, 2003, **207**, 143-154.
32. F. R. Groves, *Journal of Chemical and Engineering Data*, 1988, **33**, 136-138.
33. Z. M. Aman, E. P. Brown, E. D. Sloan, A. K. Sum and C. A. Koh, *Physical Chemistry Chemical Physics*, 2011, 19796-19806.
34. G. Zylyftari, J. W. Lee and J. F. Morris, *Chemical Engineering Science*, 2013, DOI: 10.1016/j.ces.2013.02.056, 1-52.
35. B. Tohidi, A. Danesh, A. Todd, R. Burgass and K. Østergaard, *Fluid Phase Equilibria*, 1997, **138**, 241-250.
36. J. S. Zhang and J. W. Lee, *J. Chem. Eng. Data*, 2009, **54**, 659-661.
37. P. T. Ngema, C. Petticrew, P. Naidoo, A. H. Mohammadi and D. Ramjugernath, *J. Chem. Eng. Data*, 2013, **58**, 2695-2695.
38. D. Liang, K. Guo, R. Wang and S. Fan, *Fluid Phase Equilibria*, 2001, **187-188**, 1-10.
39. C. J. Taylor, K. T. Miller, C. A. Koh and E. D. Sloan Jr., *Chemical Engineering Science*, 2007, **62**, 6524-6533.
40. S.-L. Li, C.-Y. Sun, B. Liu, X.-J. Feng, F.-G. Li, L.-T. Chen and G.-J. Chen, *AIChE Journal*, 2013, **59**, 2145-2154.
41. J. Chen, C.-Y. Sun, B. Liu, B.-Z. Peng, X.-L. Wang, G.-J. Chen, J. Y. Zuo and H.-J. Ng, *AIChE Journal*, 2012, **58**, 2216-2225.

42. L. E. Dzyaloshinskii, E. M. Lifshitz and L. P. Pitaevskii, *Soviet Physics*, 1961, **73**, 153-176.
43. M. Bienfait, *Surface Science*, 1992, **272**, 1-9.
44. D. Nenow and A. Trayanov, *Journal of Crystal Growth*, 1986, **79**, 801-805.
45. A. Pavlovska, D. Dobrev and E. Bauer, *Surface Science*, 1994, **314**, 341-352.
46. A. Doppenschmidt and H.-J. Butt, *Langmuir*, 2000, **16**, 6709-6714.
47. Y. Halpern, V. Thieu, R. W. Henning, X. Wang and A. J. Schultz, *J. Am. Chem. Soc.*, 2001, **123**, 12826-12831.
48. D. Turner and L. Talley, presented in part at the 6th International Conference on Gas Hydrates (ICGH 2008), Vancouver, BC, 2008.
49. R. Larsen, C. A. Knight and E. D. Sloan Jr, *Fluid Phase Equilibria*, 1998, **150–151**, 353-360.
50. T. Y. Makogon, R. Larsen, C. A. Knight and E. Dendy Sloan Jr, *Journal of Crystal Growth*, 1997, **179**, 258-262.
51. P. W. Wilson and A. D. J. Haymet, *Chemical Engineering Journal*, 2010, **161**, 146-150.
52. R. H. Fowler, *Proc. Roy. Soc.*, 1937, **A159**.
53. R. H. Fowler and E. A. Guggenheim, *Statistical Thermodynamics*, Cambridge Press, 1939.
54. J. Weiss, in *Current Protocols in Food Analytical Chemistry*, John Wiley & Sons, Inc., 2001, DOI: 10.1002/0471142913.fad0306s07.
55. Z. W. A, in *Contact Angle, Wettability, and Adhesion*, AMERICAN CHEMICAL SOCIETY, 1964, vol. 43, ch. 1, pp. 1-51.
56. R. Asserson, A. Hoffmann, S. Hoiland and K. Asvik, *Journal of Petroleum Science and Engineering*, 2009, **68**, 209-217.
57. S.-o. Yang, D. Kleehammer, Z. Huo, J. Sloan, E Dendy and K. Miller, *Journal of Colloid and Interface Science*, 2004, **277**, 335-341.
58. Z. M. Aman, K. Olcott, K. Pfeiffer, E. D. Sloan, A. K. Sum and C. A. Koh, *Langmuir*, 2013, **29**, 2676-2682.
59. D. Y. Kwok and A. W. Neumann, *Advances in Colloid and Interface Science*, 1999, **81**, 167-249.
60. D. Y. Kwok and A. W. Neumann, *Colloids and Surfaces A: Physicochemical and Engineering Aspects*, 2000, **161**, 31-48.
61. A. Goebel and K. Lunkenheimer, *Langmuir*, 1997, 369-372.
62. T. Uchida, T. Ebinuma, S. Takeya, J. Nagao and H. Narita, *J. Phys. Chem. B*, 2002, **106**, 820-826.
63. R. Anderson, M. Llamedo, B. Tohidi and R. W. Burgass, *J. Phys. Chem. B*, 2003, **107**, 3507-3514.
64. Y. Seo, S. Lee, I. Cha, J. D. Lee and H. Lee, *J. Phys. Chem. B*, 2009, **113**, 5487-5492.
65. C. Paull, W. S. Reeburgh, S. R. Dallimore, G. Enciso, C. A. Koh, K. A. Kvenvolden, C. Mankin and M. Riedel, *Realizing the Energy Potential of Methane Hydrate for the United States*, National Research Council of the National Academies, Washington, D.C, 2010.
66. S.-Y. Lin, K. McKeigue and C. Maldarelli, *AIChE Journal*, 1990, **36**, 1-11.
67. R. Alberty, *Langmuir*, 1995, **11**, 3598-3600.
68. F. C. Goodrich, eds. W. J. Weber and E. Matijević, American Chemical Society, WASHINGTON, D. C., 1968, vol. 79.
69. A. W. Neumann, R. David and Y. Zuo, eds., *Applied Surface Thermodynamics*, Taylor & Francis Group, Boca Raton, FL, 2010.
70. C. Lo, J. S. Zhang, P. Somasundaran, S. Lu, A. Couzis and J. W. Lee, *Langmuir*, 2008, **24**, 12723-12726.
71. C. Lo, J. Zhang, P. Somasundaran and J. W. Lee, *Journal of Colloid and Interface Science*, 2012, **376**, 173-176.
72. J. S. Zhang, C. Lo, P. Somasundaran and J. W. Lee, *Journal of Colloid and Interface Science*, 2010, **341**, 286-288.
73. T. Carver, M. Drew and P. Rodger, *J. Chem. Soc. Faraday Trans.*, 1995, **91**, 3449-3460.
74. Z. M. Aman, L. E. Dieker, G. Aspenes, A. K. Sum, E. D. Sloan and C. A. Koh, *Energy & Fuels*, 2010, **24**, 5441-5445.
75. J. Zhang, C. Lo, A. Couzis, P. Somasundaran, J. Wu and J. Lee, *J. Phys. Chem. C*, 2009, **113**, 17418-17420.
76. E. G. Dirdal, C. Arulanantham, H. Sefidroodi and M. A. Kelland, *Chemical Engineering Science*, 2012, **82**, 177-184.
77. R. Wu, Z. M. Aman, E. F. May, K. A. Kozielski, P. G. Hartley, N. Maeda and A. K. Sum, *Energy & Fuels*, 2014, **28**, 3632-3637.
78. M. Kelland, *Energy & Fuels*, 2006, **20**, 825-847.
79. E. M. Freer, M. S. Selim and E. D. Sloan, *Fluid Phase Equilibria*, 2001, **185**, 65-75.
80. R. Ohmura, S. Matsuda, T. Uchida, T. Ebinuma and H. Narita, *Crystal Growth & Design*, 2005, **5**, 953-957.
81. K. Saito, M. Kishimoto, R. Tanaka and R. Ohmura, *Crystal Growth & Design*, 2011, **11**, 295-301.
82. M. Kishimoto, S. Iijima and R. Ohmura, *Industrial & Engineering Chemistry Research*, 2012, DOI: 10.1021/ie202785z, 120328110325008.
83. A. Kumar, T. Sakpal, P. Linga and R. Kumar, *Fuel*, 2013, **105**, 664-671.
84. J. Yoslim, P. Linga and P. Englezos, *Journal of Crystal Growth*, 2010, **313**, 68-80.
85. A. K. Norland and M. A. Kelland, *Chemical Engineering Science*, 2012, **69**, 483-491.
86. J. L. Creek, S. Subramanian and D. Estanga, presented in part at the SPE Offshore Technology Conference, Mar 24, 2011.
87. D. Turner, K. Miller and E. Sloan, *Chemical Engineering Science*, 2009, **64**, 3996-4004.
88. P. G. Lafond, M. W. Gilmer, C. A. Koh, E. D. Sloan, D. T. Wu and A. K. Sum, *Phys. Rev. E*, 2013, **87**, 8.
89. A. Guariguata, M. A. Pascall, M. W. Gilmer, A. K. Sum, E. D. Sloan, C. A. Koh and D. T. Wu, *Phys. Rev. E*, 2012, **86**, 061311.
90. J. Sjöblom, B. Øvrevoll, G. Jentoft, C. Lesaint, T. Palermo, A. Sinquin, P. Gateau, L. Barré, S. Subramanian, J. Boxall, S. Davies, L. Dieker, D. Greaves, J. Lachance, P. Rensing, K. Miller, E. D. Sloan and C. A. Koh, *Journal of Dispersion Science and Technology*, 2010, **31**, 1100-1119.
91. J. Sjoblom, N. Aske, I. Auflem, O. Brandal, T. Havre, O. Saether, A. Westvik, E. Johnsen and H. Kallevik, *Advances in Colloid and Interface Science*, 2002, 399-473.
92. J. Gong, Q.-p. Li, Y. Li and D. Yu, *Journal of Hydrodynamics*, 2006, **18**, 310-314.
93. J. A. Boxall, C. A. Koh, E. D. Sloan, A. K. Sum and D. T. Wu, *Langmuir*, 2012, **28**, 104-110.
94. A. Kolmogorov, *Dok. Akad. Nuak*, 1949, **66**, 825-828.
95. J. O. Hinze, *AIChE Journal*, 1955, **1**, 289-295.
96. J. J. M. Janssen, A. Boon and W. G. M. Agterof, *Colloids and Surfaces A: Physicochemical and Engineering Aspects*, 1994, **91**, 141-148.

97.   N. Vankova, S. Tcholakova, N. D. Denkov, I. B. Ivanov, V. D. Vulchev and T. Danner, *Journal of Colloid and Interface Science*, 2007, **312**, 363-380.

98.   A. Haber, M. Akhfash, K. Loh, Z. M. Aman, E. O. Fridjonsson, E. F. May and M. L. Johns, *Langmuir*, 2015, **31**, 8786–8794.

99.   S. R. Davies, E. D. Sloan, A. K. Sum and C. A. Koh, *J. Phys. Chem. C*, 2010, **114**, 1173-1180.

100.   S. Middleman, *Industrial & Engineering Chemistry Process Design and Development*, 1974, **13**, 78-83.

101.   A. Cameirao, A. Fezoua, Y. Ouabbas, J.-M. Herri, M. Darbouret, A. Sinquin and P. Glenat, presented in part at the 7th International Conference on Gas Hydrates, Edinburgh, 2011.

102.   A. A. Potanin, *Journal of Colloid and Interface Science*, 1991, **145**, 140-157.

103.   K. Mühle, *Colloids and Surfaces*, 1987, **22**, 1-21.

104.   K. Mühle, in *Theory and Applications*, ed. B. Dobias, Marcel Dekker, Inc., New York, First Edition edn., 1993.

105.   A. Sinquin, T. Palermo and Y. Peysson, *Oil & Gas Science and Technology*, 2004, **59**, 41-57.

106.   P. Mills, *Journal de Physique Lettres*, 1985, **46**, 301-309.

107.   P. K. Senapati, D. Panda and A. Parida, *Journal of Minerals & Materials Characterization & Engineering*, 2009, **8**, 203-221.

108.   J. Mcculfor, P. Himes and M. R. Anklam, *AIChE Journal*, 2010, **57**, 2334-2340.

109.   R. Camargo and T. Palermo, presented in part at the 4th International Conference on Gas Hydrates, Jun 19, 2002.

110.   E. B. Webb, P. J. Rensing, C. A. Koh, E. D. Sloan, A. K. Sum and M. W. Liberatore, *Energy & Fuels*, 2012, **26**, 3504-3509.

111.   J. Israelachvili, *Intermolecular & Surface Forces*, Academic Press, Great Britain, Second Edition edn., 1991.

112.   K. L. Johnson, K. Kendall and A. D. Roberts, *Proceedings of the Royal Society of London A: Mathematical, Physical and Engineering Sciences*, 1971, **324**, 301-313.

113.   B. V. Derjaguin, V. M. Muller and Y. P. Toporov, *Journal of Colloid and Interface Science*, 1975, **53**, 314-326.

114.   C. D. Willett, M. J. Adams, S. a. Johnson and J. P. K. Seville, *Langmuir*, 2000, **16**, 9396-9405.

115.   H. Schubert, *Powder Technology*, 1984, **37**, 105-116.

116.   Y. I. Rabinovich, M. S. Esayanur, K. D. Johanson, J. J. Adler and B. M. Moudgil, *Journal of Adhesion Science and Technology*, 2002, **16**, 1-18.

117.   Y. Rabinovich, M. Esayanur and B. Moudgil, *Langmuir*, 2005, **21**, 10992-10997.

118.   F. E. Kruis, K. A. Kusters, S. E. Pratsinis and B. Scarlett, *Aerosol Science and Technology*, 1993, **19**, 514-526.

119.   L. E. Dieker, Z. M. Aman, N. C. George, A. K. Sum, E. D. Sloan and C. A. Koh, *Energy & Fuels*, 2009, **23**, 5966-5971.

120.   C. Taylor, M.S., Colorado School of Mines, 2006.

121.   T. Uchida, T. Shiga, M. Nagayama and K. Gohara, *Energies*, 2010, **3**, 1960-1971.

122.   B. R. Lee, C. A. Koh and A. K. Sum, *Review of Scientific Instruments*, 2014, **85**, 095120.

123.   N. Maeda, Z. M. Aman, K. A. Kozielski, C. A. Koh, E. D. Sloan and A. K. Sum, *Energy & Fuels*, 2013, **27**, 5168-5174.

124.   S. Davies, J. Boxall, C. Koh, E. D. Sloan, P. Hemmingsen, K. Kinnari and Z.-G. Xu, *SPE Production & Operations*, 2009, 1-6.

125.   J. Peixinho, P. U. Karanjkar, J. W. Lee and J. F. Morris, *Langmuir*, 2010, **26**, 11699-11704.

126.   Z. M. Aman, K. Pfeiffer, S. J. Vogt, M. L. Johns and E. F. May, *Colloids and Surfaces A: Physicochemical and Engineering Aspects*, 2014, **448**, 81-87.

127.   L. E. Zerpa, Z. M. Aman, S. Joshi, I. Rao, E. D. Sloan, C. A. Koh and A. K. Sum, presented in part at the SPE Offshore Technology Conference, Houston, 2012.

128.   T. J. Danielson, presented in part at the SPE Offshore Technology Conference, Houston, TX, 2011.

129.   T. J. Danielson, K. M. Bansal, B. Djoric, D. Larrey, S. T. Johansen, A. De Leebeeck and J. Kjølaas, presented in part at the SPE Offshore Technology Conference, 2012.

130.   M. Di Lorenzo, Z. M. Aman, G. Sanchez Soto, M. L. Johns, K. A. Kozielski and E. F. May, *Energy & Fuels*, 2014, **28**, 3043–3052.

131.   M. Di Lorenzo, Z. M. Aman, K. Kozielski, B. W. E. Norris, M. L. Johns and E. F. May, *Energy & Fuels*, 2014, **28**, 7274–7284.

132.   J. W. Lachance, L. D. Talley, D. P. Shatto, D. J. Turner and M. W. Eaton, *Energy & Fuels*, 2012, **26**, 4059-4066.

133.   J. W. Nicholas, L. E. Dieker, E. D. Sloan and C. A. Koh, *Journal of Colloid and Interface Science*, 2009, **331**, 322-328.

134.   G. Aspenes, L. E. Dieker, Z. M. Aman, S. Høiland, A. K. Sum, C. A. Koh and E. D. Sloan, *Journal of Colloid and Interface Science*, 2010, **343**, 529-536.

135.   O. C. Hernandez, University of Tulsa, Ph.D. Thesis, 2006.

136.   S. V. Joshi, G. A. Grasso, P. G. Lafond, I. Rao, E. Webb, L. E. Zerpa, E. D. Sloan, C. A. Koh and A. K. Sum, *Chemical Engineering Science*, 2013, **97**, 198–209.

137.   Z. M. Aman, S. E. Joshi, E. D. Sloan, A. K. Sum and C. A. Koh, *Journal of Colloid and Interface Science*, 2012, **376**, 283-288.

138.   E. D. Sloan, S. Subramanian, P. N. Matthews, J. P. Lederhos and A. A. Khokhar, *Ind. Eng. Chem. Res*, 1998, **37**, 3124-3132.

139.   A. Lone and M. A. Kelland, 2013, **27**, 2536-2547.

140.   N. Maeda, *Review of Scientific Instruments*, 2014, **85**, 065115.

141.   J. H. K. Song, A. Couzis and J. W. Lee, *Langmuir*, 2010, **26**, 18119-18124.

142.   H. Sakaguchi, R. Ohmura and Y. H. Mori, *Journal of Crystal Growth*, 2003, **247**, 631-641.

143.   M. Zanota, C. Dicharry and A. Graciaa, *Energy & Fuels*, 2005, **19**, 584-590.

144.   Z. Huo, E. Freer, M. Lamar, B. Sannigrahi, D. Knauss and E. D. Sloan, *Chemical Engineering Science*, 2001, **56**, 4979-4991.

145.   J. York and A. Firoozabadi, *J. Phys. Chem. B*, 2008, **112**, 10455-10465.

146.   J. York and A. Firoozabadi, *Energy & Fuels*, 2009, **23**, 2937-2946.

147.   P. Webber, presented in part at the SPE Offshore Technology Conference, 2010.

148.   C. Angle and J. Sjoblom, *Encyclopedic Handbook of Emulsion Technology*, 2001.

149. Y. Fan, S. b. Simon and J. Sjoblom, *Energy & Fuels*, 2009, **23**, 4575-4583.

150. M. Sun and A. Firoozabadi, *Journal of Colloid and Interface Science*, 2013, **402**, 312-319.

151. S. Gao, *Energy & Fuels*, 2009, **23**, 2118-2121.

152. L. E. Zerpa, J.-L. Salager, C. A. Koh, E. D. Sloan and A. K. Sum, *Industry & Engineering Chemistry Research*, 2010, **50**, 188-197.

153. A. Borgund, S. Hoiland, T. Barth, P. Fotland, R. Kini and R. Larsen, presented in part at the 6th Internatioanl Conference on Gas Hydrates (ICGH 2008), Jul 01, 2008.

154. A. Borgund, S. Høiland, T. Barth, P. Fotland and K. Askvik, *Applied Geochemistry*, 2009, **24**, 777-786.

155. J. Clemente, N. Prasad, M. MacKinnon and P. Fedorak, *Chemosphere*, 2003, **50**, 1265-1274.

156. J. Clemente and P. Fedorak, *Chemosphere*, 2005, **60**, 585-600.

157. K. Erstad, S. Hoiland, P. Fotland and T. Barth, *Energy & Fuels*, 2009, **23**, 2213-2219.

158. K. Erstad, S. Hoiland, T. Barth and P. Fotland, presented in part at the 6th International Conference on Gas Hydrates (ICGH 2008), Jul 01, 2008.

159. T. Barth, S. Hoiland, P. Fotland, K. Askvik, B. Pedersen and A. Borgund, *Organic Geochemistry*, 2004, **35**, 1513-1525.

160. G. Genov, E. Nodland, B. B. Skaare and T. Barth, *Organic Geochemistry*, 2008, **39**, 1229-1234.

161. W. Meredith, S.-J. Kelland and D. Jones, *Organic Geochemistry*, 2000, **31**, 1059-1073.

162. J. R. Gasson, T. Barth and G. Genov, *Journal of Petroleum Science and Engineering*, 2013, **102**, 66-72.

163. A. Fafet, F. Kergall, M. Silva and F. Behar, *Organic Geochemistry*, 2008, **39**, 1235-1242.

164. M. Barrow, L. McDonnell, X. Feng, J. Walker and P. Derrick, *Anal. Chem.*, 2003, **75**, 860-866.

165. J. Headley, K. Peru and M. Barrow, *Mass Spectrometry Reviews*, 2009, **28**, 121-134.

166. E. Norgard and J. Sjoblom, *Journal of Dispersion Science and Technology*, 2008, **29**, 1114-1122.

167. E. Norgard, H. Magnusson, A.-M. Hanneseth and J. Sjoblom, *Colloids and Surfaces A: Physicochemical and Engineering Aspects*, 2009, **340**, 99-108.

168. J. Sjöblom, S. Simon and Z. Xu, *Advances in Colloid and Interface Science*, 2014, **205**, 319-338.

169. B. Smith, P. Sutton, C. Lewis, B. Dunsmore, G. Fowler, J. Krane, B. Lutnaes, O. Brandal, J. Sjoblom and S. Rowland, *J. Sep. Sci*, 2007, **30**, 375-380.

170. G. Flatabø, 2013.

171. Z. M. Aman, Colorado School of Mines, 2012.

172. S. Standal, A. Blokhus, J. Haavik, A. Skauge and T. Barth, *Journal of Colloid and Interface Science*, 1999, **212**, 34-41.

173. S. Standal, J. Haavik, A. M. Blokhus and A. Skauge, *Journal of Petroleum Science and Engineering*, 1999, **24**, 131-114.

174. Z. M. Aman, E. D. Sloan, A. K. Sum and C. A. Koh, *Energy & Fuels*, 2012, **26**, 5102-5108.

175. S. Lang, *Current Opinion in Colloid & Interface Science*, 2002, **7**, 12-20.

176. P. Le Parlouër, C. Dalmazzone, B. Herzhaft, L. Rousseau and C. Mathonat, *Journal of Thermal Analysis and Calorimetry*, 2004, **78**, 165-172.

177. M. Akhfash, J. A. Boxall, Z. M. Aman, M. L. Johns and E. F. May, *Chemical Engineering Science*, 2013, **104**, 177-188.

178. D. Greaves, J. Boxall, J. Mulligan, E. D. Sloan and C. A. Koh, *Chemical Engineering Science*, 2008, **63**, 4570-4579.

179. D. Dalmazzone, C. Dalmazzone and B. Herzhaft, *SPE Journal*, 2002.

180. F. Ning, L. Zhang, Y. Tu, G. Jiang and M. Shi, *Journal of Natural Gas Chemistry*, 2010, **19**, 234-240.

181. J. Lachance, E. D. Sloan and C. A. Koh, *Chemical Engineering Science*, 2008, **63**, 3942-3947.

182. X. Lv, B. Shi, Y. Wang and J. Gong, 2013, DOI: 10.1021/ef401648r, 131126073616005.

183. H. Leba, A. Cameirao, J.-M. Herri, M. Darbouret, J.-L. Peytavy and P. Glenat, *Chemical Engineering Science*, 2010, **65**, 1185-1200.

184. E. Colombel, P. Gateau, L. Barré, F. Gruy and T. Palermo, *Oil & Gas Science and Technology - Revue de l'IFP*, 2009, **64**, 629-636.

185. Z. M. Aman, E. D. Sloan, A. K. Sum and C. A. Koh, *Physical Chemistry Chemical Physics*, 2014, **16**, 25121-25128.

186. J. D. Smith, A. J. Meuler, H. L. Bralower, R. Venkatesan, S. Subramanian, R. E. Cohen, G. H. McKinley and K. K. Varanasi, *Physical Chemistry Chemical Physics*, 2012, **14**, 6013.